EFB Bioeconomy Journal 2 (2022) 100025

Contents lists available at ScienceDirect

EFB Bioeconomy Journal

journal homepage: www.elsevier.com/locate/bioeco

Studying the application of fish-farming net-cleaning waste as fire-retardant for Scots pine (*Pinus sylvestris* L.) sapwood

Edita Garskaite[a,*], Maria M. Estevez[b], Alexandra Byström[c], Michael Försth[c], Zivile Stankeviciute[d], Denis Sokol[d], Matthew Steele[e], Dick Sandberg[a]

[a] Wood Science and Engineering, Department of Engineering Sciences and Mathematics, Luleå University of Technology, Forskargatan 1, SE-931 87 Skellefteå, Sweden
[b] Aquateam COWI AS, Karvesvingen 2, Oslo NO-0572, Norway
[c] Structural and Fire Engineering, Department of Civil, Environmental and Natural Resources Engineering, Luleå University of Technology, SE-977 54 Luleå, Sweden
[d] Institute of Chemistry, Faculty of Chemistry and Geosciences, Vilnius University, Naugarduko 24, Vilnius LT-03225, Lithuania
[e] Delong America, 4020 Rue St. Ambroise, Suite 473, Montreal H4C 2C7, Canada

ARTICLE INFO

Keywords:
Scots pine wood
Aquaculture waste
TG-FTIR gas
SEM/EDX
XRD
Cone calorimeter

ABSTRACT

Optimising the exploitation of available waste resources for the recovery of their intrinsic value will be vital in the future circular economy society. Recovery of energy, nutrients and metals from waste streams is in focus today. This study aimed to evaluate the use of an aquaculture waste, i.e. the dried-solid waste discharge that generates by cleaning the fishing-nets, as a potential fire-retardancy promoter for Scots pine sapwood. As-received dried-solid waste from salmon-farming was calcined at different temperatures to evaluate material phase transformation and achieve homogeneous phase distribution. Thermal degradation of waste powders was studied by TG-FTIR gas analysis when annealing the material to temperatures up to 800°C, and the crystallinity, phase composition, morphology, elemental composition and particle sizes of as-received and calcined-waste materials at different temperatures were evaluated by XRD, FTIR, SEM/EDS, and TEM analyses. The flammability studies using cone calorimeter of Scots pine sapwood blocks treated with as-received and processed material is also reported and discussed. Results were promising, indicating that the aquaculture waste could be employed as an effective fire-retardant. The possibility of value-creation from waste discharges is enforced in this study so to promote the way towards waste valorisation and circular economy.

1. Introduction

Today's circular economy demands innovative solutions to help exploit all the value that lies within the waste streams that society generates, and thus to switch the concept of waste into a resource. At places as western Norway the availability of waste resources coming from the aquaculture and fish-processing sectors, is relevant for implementing revalorisation processes (Carballeira Braña et al., 2021; Ishita et al., 2020). It is expected that the amount of farmed fish in Norway will increase fivefold by the year 2050 (Bailey and Eggereide, 2020). The western region shows an increased number of on-land aquaculture farms as well and of recirculation systems producing more amount of fish sludge which demands sustainable solutions to enhance waste management and the recycling of resources. The sector is under pressure due to the need to achieve significant reduction in nutrient discharge to the fjords in the region; there is insufficient water available locally to accommodate such high discharge, and employment of fish waste/sludge as fertilizer competes for land with the animal manure application in such high-density cattle production region. In fact, the application of phosphorus (P)-rich materials to soil in such region often exceeds crop P-requirements. The resulting soil-P accumulation increases the risk of P losses to waterways through erosion and run-off (Hanserud et al., 2017). In addition, restrictions towards P-spreading are being considered by the Norwegian Government (Norwegian Agriculture Agency, 2018) and estimated to take place in the short future, directing the need of handling nutrient-rich waste streams into other sustainable solutions than producing fertiliser.

Fish waste can be categorized either as the material coming from the slaughter of fish in vessels or processing plants (heads, viscera, backbones, cuts and rejected fish from processing) that can be used further for feed production, and the material with risks of fish diseases and/or with residues of drugs content over the limit, that must be hygienised and subsequently treated using alternative methods as composting or biogas production (Norwegian Scientific Committee for Food Safety, 2010; Estevez et al., 2014). An additional type of fish-waste are

* Corresponding author.
E-mail address: edita.garskaite@ltu.se (E. Garskaite).

https://doi.org/10.1016/j.bioeco.2022.100025
Received 11 December 2021; Received in revised form 20 February 2022; Accepted 9 March 2022

the discharges from the procedures of net-washing and cleaning, consisting mainly of inorganic compounds and some biomass residues.

For energy production, fish waste streams are very energetic and can complement the processes of sludge or animal manure digestion (Hanserud et al., 2017; Estevez et al., 2014; Bloecher and Floerl, 2021). However, the heavy metals content in fish waste streams may concentrate under organic matter degradation processes as anaerobic digestion and composting, leading to higher concentrations of metals in the final solid product obtained (per gram of dried product) (Bloecher and Floerl, 2021; Bannister et al., 2019). If the aim is to apply such final product as fertiliser, restrictions regarding heavy metal content in fertilisers from organic origin (Norwegian Food Safety Authority, 2019) will limit the use when/if fish waste streams are used as the processes-feedstock. Thus, novel applications for such waste streams have to be considered.

Regarding net-cleaning processes, biofouling, the growth of organisms on the submerged net structures, is a serious challenge for global marine salmon aquaculture, impairing farming operations, fish health and welfare (Bloecher and Floerl, 2021; Bannister et al., 2019; Comas et al., 2021). Furthermore, maintenance due to the accumulation of organic-inorganic deposits on the net structures leads to high costs and time-consuming processes. The deposit-mixture contains different metals, with copper being one of the main elements. It comes from the antifouling paints where copper (I) oxide (Cu_2O) is used as biocidal agent (Bloecher and Floerl, 2021, Bloecher and Floerl, 2020; Braithwaite et al., 2007). Thus, such discharged material is considered a hazardous waste. During the successive net post-cleaning and waste material-treatment the copper is extracted from discharged material, but the challenges associated with the cost-effective and sustainable utilization of waste originating from marine fish-farming industry still remains. Therefore, research on applicable and practical valorisation solutions for the waste generated by the aquaculture and fisheries-sector that considers the "metal load" of the waste are needed.

With respect to the waste streams containing inorganic compounds as metals have a value for themselves, such "metal load" is a valuable source of different materials which could be explored as a fire-retardancy promoter/enhancer for wood and wood products. Wood is seen as a carbon neutral material regarding climate emissions (Lippke et al., 2010), and new technologies, mass-timber systems and environmental benefits bring an increasing interest in timber buildings world-wide. Regulations require that such wooden structures meet prescribed performance for fire-resistance (Östman, 2021).

The flammability of wood and wood-based products can be altered by chemical means using fire retardants, and the conventional wood fire-retardant processing techniques involve vacuum-pressure impregnation or applying fire-proof coatings to the wood surface without modifying the intrinsic properties of the material (Popescu and Pfriem, 2019; Lowden and Hull, 2013; Lazar et al., 2020). The vacuum-pressure impregnation usually proceeds from aqueous solutions that easily diffuse into the wood matrix. Studies showed that many compounds containing B, P, Al, and N are to be effective fire retardants (Popescu and Pfriem, 2019; Lowden and Hull, 2013). Nevertheless, even though the variety of additives were proposed and are used as fire-retardant materials, the challenges such as leachability of the additives and toxicity considerations to human health and environment still remain (Popescu and Pfriem, 2019; Östman and Tsantaridis, 2017). The leakage of fire-retardant additives when the wood products are exposed to elevated moisture conditions could lead to a decreased fire-retardancy effect. As a result, the safety of the building's occupants during a fire event can be compromised.

Oxides of Si, Mg, Ca, Fe and Cu were also studied as fire retardants (Hamdani et al., 2009; Chen and Wang, 2010; Laoutid et al., 2021). Metals or metal oxides are supposed to absorb heat and act as flame-suppressing materials. Many attempts were made to explore synergistic effects of different inorganic and organic materials properties. For example, Cu_2O was demonstrated to exhibit synergistic effects with ammonium polyphosphate, on improving the flame retardancy and smoke suppression of epoxy resin (Chen et al., 2015). $CuMoO_4$ oxide also showed smoke suppression and flame retardancy effects on polymeric materials (Xu et al., 2018). In another study, fire-retardancy of plastics was enhanced when nanometric Fe_2O_3 was embedded within polymeric matrix (Gallo et al., 2011).

In this work, the application of the dried, solid fish-farming waste material was evaluated as a fire-retardancy promoter for Scots pine sapwood by performing thermal degradation of the waste and an analysis of the gas composition via TG-FTIR in addition to phase and elemental composition analysis, crystallinity and morphology. The flammability of Scots pine sapwood treated with as-received and calcined aquaculture waste material was evaluated performing cone calorimeter test. Preliminary results indicate the potential pathway towards responsible use of materials, cost-effective and environmentally sustainable solutions.

2. Experimental

2.1. Preparation of oxide-based powders

The initial powdered material from the fish farming industry (Egersund Net, AKVA group, Norway) was processed at 55-60 °C in the bioreactors by Global Enviro, Norway, and is designated herein as an as-received waste. This obtained as-received aquaculture waste was calcined for 3 hours at 350 °C and 550 °C (ramp-up rate 5 °C/min.) in order to decompose the organics in the material. Calcined powders were then ground in a mortar and fraction of this material was then further calcined for 3 hours at 900 °C (ramp-up rate 5 °C/min.). Annealed material was additionally ground in a mortar.

2.2. Wood processing and treatment with aquaculture waste

Specimens of Scots pine (*Pinus sylvestris* L.) sapwood having sizes of 10 × 10 × 1 cm (Tangential (T) × Radial (R) × Longitudinal (L)) were cut from sawn timber obtained from northern Sweden. Powders of the processed aquaculture waste material were then deposited on the sapwood blocks rubbing them mechanically into the surface to saturate micropores of the wood surface. The average mass increase of the wood blocks was 0.1 ± 0.04 wt.% and 0.25 ± 0.12 wt.% for the as-received waste material and that which was annealed at 550°C, respectively. Specimens were then conditioned in a climate chamber (20 °C, 65% relative humidity (RH)) for 5 days.

2.3. Characterisation

Thermal behaviour of as-received material from the fish farming industry was evaluated by performing thermogravimetry (TG) coupled with the Fourier transform infrared (FT-IR) spectroscopy. PerkinElmer TGA 4000 instrument was employed. The weight of specimens was about 6 mg. The specimens were heated from 30°C to 800°C with a constant rate of 10 °/min and held at 820°C for 10 min. The purge gas through the TG was nitrogen (flow supply 2 bar). FT-IR spectrometer (Frontier FT-IR, Perkin Elmer, DTGS detector) equipped with a gas flow cell (the temperature for gas flow cell and transfer line was 275 °C, nitrogen gas flow rate was 20 mL/min.) was used in conjunction with TG analysis to record infrared (IR) absorption spectra of volatile components evolved from the sample. IR spectra over the range of 4000-450 cm^{-1} were collected every 6 s at 8 cm^{-1} resolution. Spectrum TimeBase software was used for analysis of the time-resolved IR data. FTIR spectra of the homogeneously mixed wood powders of the pure and modified wood were recorded using the same FT-IR spectrometer (ZnSe/Diamond ATR crystal, DTGS detector, 4000-600 cm^{-1}, 4 scans). The morphological features of the as-received and calcined waste material were evaluated by using field emission scanning electron microscope (FE-SEM, SU-70, Hitachi) and the electron beam acceleration voltage was 5 kV. A table-top scanning electron microscope (SEM, TM3000, Hitachi, 15.0 kV acceleration voltage) was used to estimate the elemental composition of

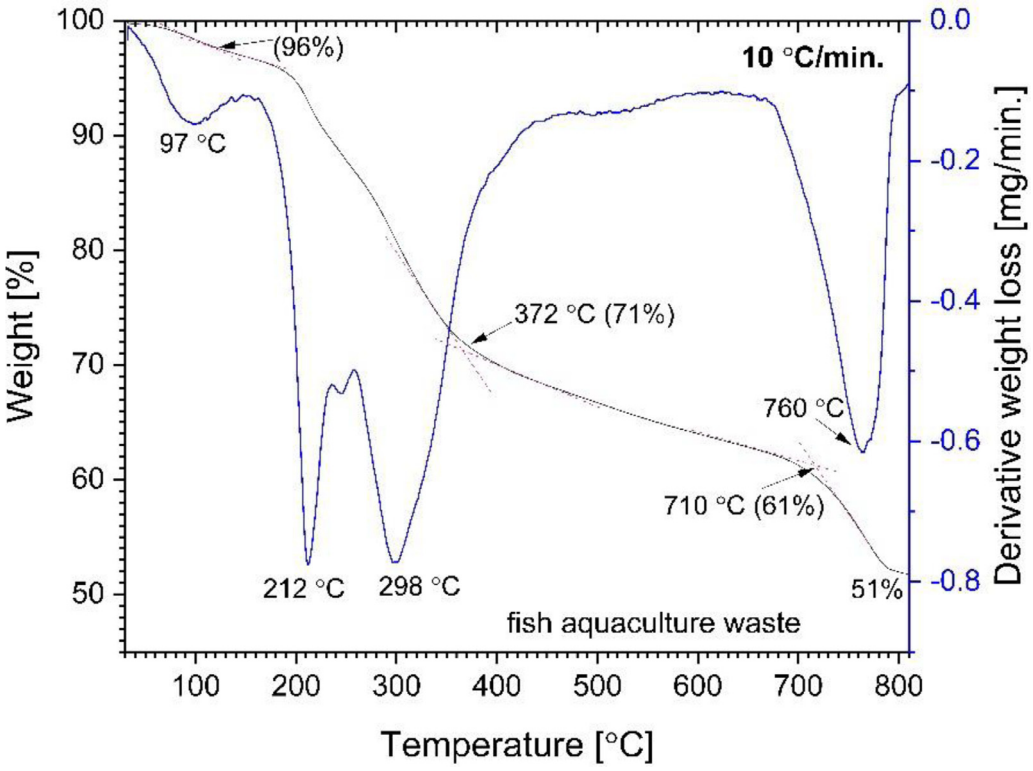

Fig. 1. Percent weight-loss curve and derivative profile versus temperature for the solid waste powders.

waste material. An X-ray acquisition time of 300 s was used to obtain the EDS spectra (n = 3 for each feature of interest). The phase composition of inorganic waste material was studied by X-ray diffraction (XRD, Rigaku, MiniFlex II, Cu-Kα radiation, λ = 0.1542 nm, 40 kV, 100 mA, 2θ = 10-70°) analysis. Transmission electron microscopy analysis of calcined powders was performed on a LVEM25 (Delong America, Montreal, Canada) transmission electron microscope (TEM) instrument. Samples were prepared for TEM measurements by drop casting suspension of material, that was sonicated for 5 min in ethanol, on carbon-coated copper TEM grids.

2.4. Cone calorimeter studies

Fire properties were measured with an ISO 5660 Cone Calorimeter from Fire Testing Technology. In the tests specimens of area 0.1 m × 0.1 m (length × width) were exposed to irradiation of 34.9 kW/m^2. The thickness of the specimens varied between 10.14 to 10.48 mm (average value of 10.29 mm). The heat release rate (HRR) was determined by measurements of the oxygen consumption derived from the oxygen concentration and the flow rate in the exhaust duct (Huggett 1980). The specimens were placed on a load cell during testing.

3. Results and discussion

3.1. Biomass characterisation

The thermal behaviour of solid biomass from aquaculture was evaluated simultaneously performing TG and FTIR gas analyses. TG and derivative thermogravimetric (DTG) curves of biomass are presented in Fig. 1, where the decomposition curves show five main steps of weight loss leaving about 51% of residue at about 780°C. The first weight loss of 4% was observed by heating the sample up to 108°C (maxima at 97°C, DTG curve) and was signed to the removal of absorbed water. The second step of ~ 2% up to 200°C could be assigned to the bound water, CO_2, and other volatile low molecular compounds that might be present in the biomass. The third, most significant, step of weight loss of 25% was observed in the range of 200-370°C (maxima in DTG 212°C and 298°C). This loss can be attributed to the degradation of organics and further release molecular species originating from organics and bio-polymers (Skvorčinskienė et al., 2019; Eimontas et al., 2021). The fourth loss of 10% and the fifth loss of 10% occurred upon material further heating up to 700°C and 780°C, respectively. These events could be related to the further degradation of organics as well as to the decomposition and phase transformation of the carbonate containing inorganic materials (Skvorčinskienė et al., 2019; Khiari et al., 2019; Rodriguez-Navarro et al., 2009).

Fig. 2 shows Gram-Schmidt (GS) profile derived from IR plots of as-received waste material that was heated at 10°C /min. between 30°C and 800°C and IR absorption spectra obtained at 19, 27 and 72 min. after the measurements. The data are in good agreement with the TGA (Fig. 1) showing that three major periods of weight loss were observed, which were associated with organic matter pyrolysis and decomposition of material upon annealing at higher temperatures. The very small signals observed in the GS plot (Fig. 2a) around 5 min. (80-90°C) result from the H_2O and CO_2 molecules evolving from the material. The intense signals in the GS plot at about 220°C and 300°C are associated with the multiple gas evolution corresponding to the initial pyrolysis of various organics and bio-polymers Fig. 2.b shows linked IR spectra of gases evolved at the times when the maxima absorption occurs for the waste sample investigated. One can observe that gas IR spectra rising after 19 min. and 27 min. show molecular components of CO_2, H_2O, SO_2 and bands which could be assigned to the components containing C–H and N–H bonds (Eimontas et al., 2021). The band at ~1750 cm^{-1} could be assigned to carbonyl (C=O) stretching vibrations of carboxyl (COO^-) group, that is present in lipids and fatty acids (Vongsvivut et al., 2012), as well as C=O functional groups of nylon (Skvorčinskienė et al. 2019). Furthermore, bands observed in 2950-2800 cm^{-1} region were assigned to the C–H vibrations, and these confirm presence of the caprolactame originating from nylon net fibers within waste material (Skvorčinskienė et al., 2019). Similar volatile compounds that were assigned to the

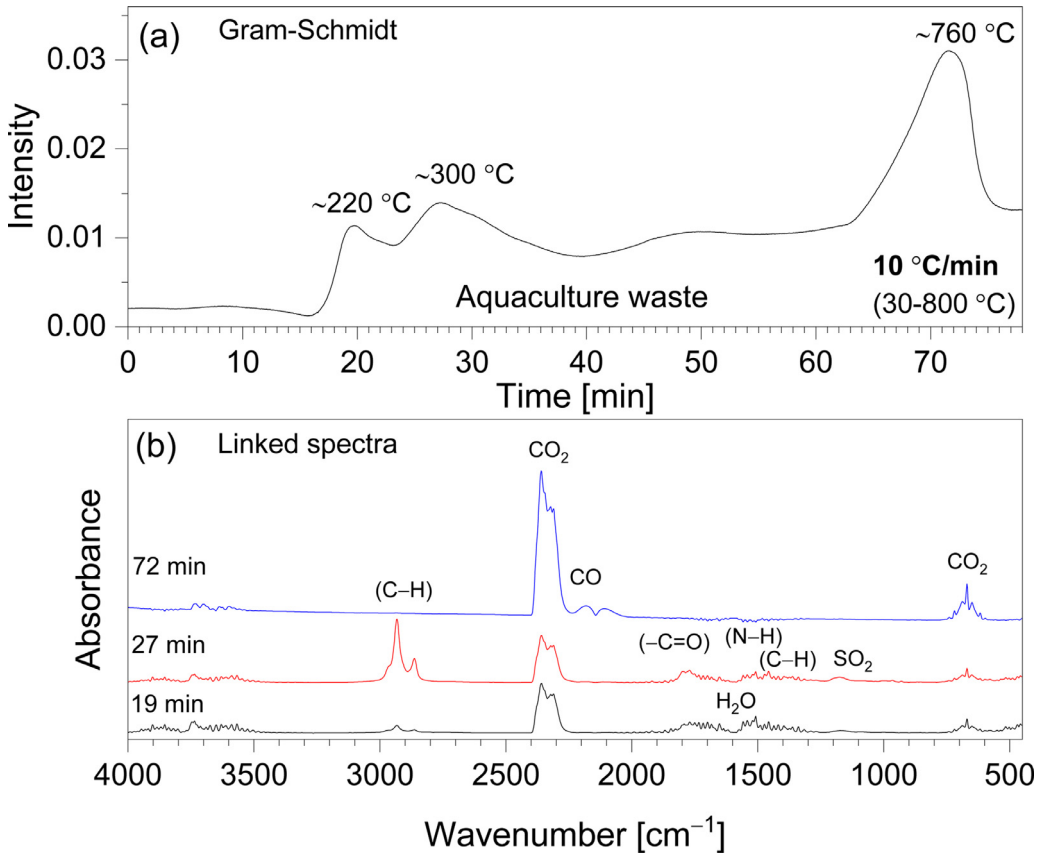

Fig. 2. (a) Gram-Schmidt profiles for solid aquaculture waste heated at 10 ºC/min between 30°C and 800°C, and (b) extracted FTIR absorbance spectra of volatile components at the maxima absorption from Gram-Schmidt plots.

functional groups of nylon material were also detected in FTIR gas spectra by Eimontas *et al.* where the catalytic pyrolysis of waste of fishing nets material was studied for the recovery of caprolactam (Eimontas et al., 2021). The IR absorbance spectrum recorded at 72 min. (strong signal in GS plot at around 760°C (Fig. 2a)) showed peaks of molecular CO_2, CO and H_2O, which can be attributed to the decomposition of inorganic material of $CaCO_3$ and calcium phosphates – these originate most likely from the inorganic matter of residues from fish shells and shells from crustations or other carbonate containing materials that could be present within waste material.

To remove residues of organic matter and evaluate transformation of inorganic phase as-received fish-farming waste was calcined at different temperatures Fig. 3. shows FTIR spectra of the initial material and that which was calcined at 550°C and 900°C. One can observe that IR spectrum of as-received material exhibit absorption bands characteristic to the organic materials, that are present within solid material as biomass fraction from fish residue. The spectrum shows broad absorption bands around 3600-3170 cm^{-1} region that arise from N–H stretching vibrations of NH_2 group present in amines and amides (Kim et al., 2005; Skvorčinskienė et al., 2019). In this region, the O–H stretching vibrations, with contributions from any bound water in the sample, also appear. The bands observed in 2950-2800 cm^{-1} (maxima at 2918 cm^{-1} and 2850 cm^{-1}) region could be attributed to the C–H deformation. Kannan *et al.* reported similar spectral features of seafood waste residue (Kannan et al., 2015). Broad bands in the 1670-1520 cm^{-1} region are characteristic vibrations of amide I and amide II, and band with a maximum at 1243 cm^{-1} could be assigned to the amide III in proteins of fish residue (Cebi et al., 2016). A strong band with maximum at 1741 cm^{-1} could be ascribed to the carbonyl (C=O) group stretching vibrations of caprolactame, a residue of polymeric material of the fishing nets (Skvorčinskienė et al., 2019; Kim et al., 2005). Furthermore, a broad overlapping peak at ~1640 cm^{-1} is due to NH_2 scissors (amides), with contribution from O–H bending modes, and the peak with maximum at 1463 cm^{-1} could be assigned to C–N stretching modes. The broad band at 1029 cm^{-1} with shoulder at 1074 cm^{-1} is characteristic to the stretching mode of P–O bond of phosphate (PO_4^{3-}) group (Garskaite et al., 2014; Uskoković et al., 2018), and so indicating the presence of fish shells and shells from crustations. In this region stretching vibrations of Si–O bands also appear (Vidal et al., 2016).

Waste powders calcined at 550°C and 900°C exhibited different spectral features, there were no bands characteristic to the organic matter in the spectra, and only those arising due to the inorganic material were observed. The most intense absorption bands in the spectrum of material annealed at 550°C were observed in the 1190-900 cm^{-1} region (bands located at ~ 956, 1033, 1084 and 1156 cm^{-1}) and were assigned to the vibrations of phosphate (PO_4^{3-}) functional groups. These absorption bands correspond to the triply degenerate asymmetric stretching mode, ν_3, and symmetric stretching mode, ν_1, of the P–O bonds of PO_4^{3-} group (Uskoković et al., 2018). The band at 956 cm^{-1} is a symmetric stretching mode of PO_4^{3-} group (P–O bond). In the 1310-1550 cm^{-1} region, overlapping bands characteristic to the carbonate (CO_3^{2-}) group appears (stretching and bending modes of the C–O bond) (Garskaite et al., 2014; Ihli et al., 2014). A strong band at 872 cm^{-1} could be also assigned to bending modes O–C–O bond of the CO_3^{2-} group (Garskaite et al., 2014), and the band present at 714 cm^{-1} is characteristic to calcite (Bosch Reig et al., 2002). Studies showed that materials containing carbonate ions have a positive effect on fire-retardancy. For instance, improved fire-retardant properties of calcified spruce and beech wood when $CaCO_3$ was mineralized within the wood cell walls using the alkaline hydrolysis of dimethyl carbonate precursors in the presence of calcium ions at ambient temperatures was demonstrated (Merk et al., 2015). In another study, improved fire-retardancy of the wood was shown when an *in-situ*

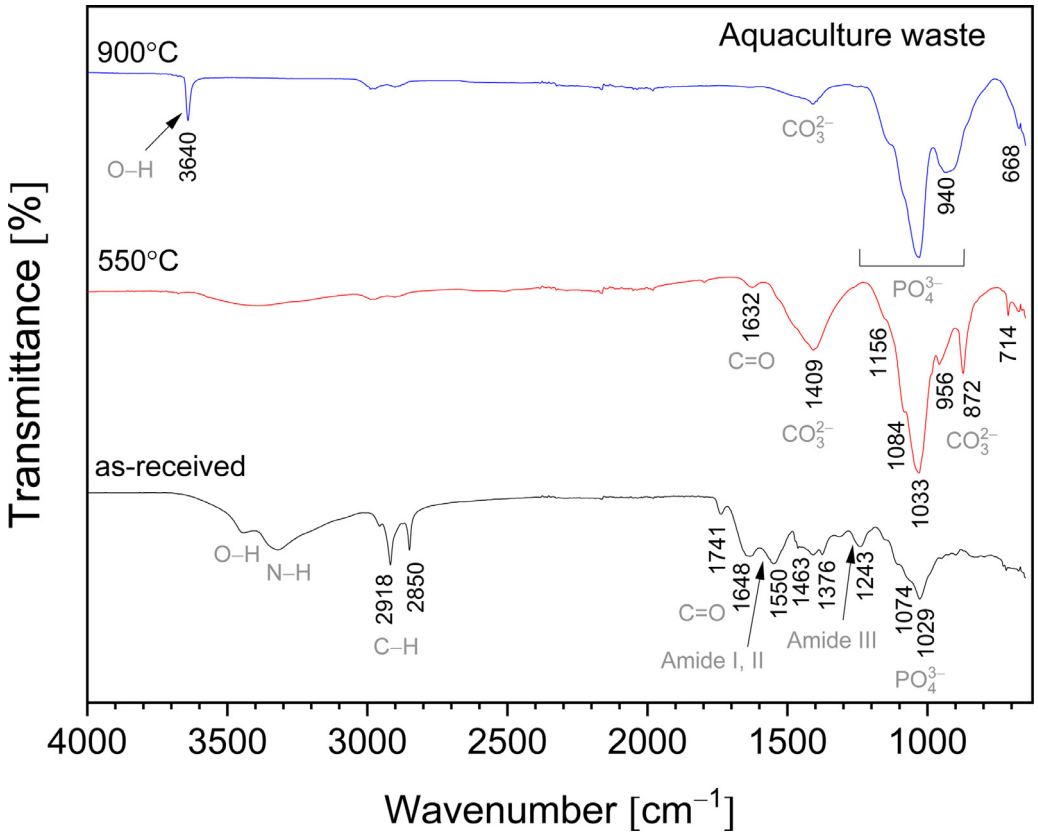

Fig. 3. FTIR spectra of as-received aquaculture waste and calcined at 550°C and 900°C.

formation of $CaCO_3$ was achieved by using a one-component treatment medium – a water solution of calcium acetoacetate (Pondelak et al., 2021). This further suggests that components of the aquaculture-waste inorganic materials could be considered an important additive to the fire retardant systems at aiming to solve the problems of flammability and environmental safety.

The spectrum of waste powders calcined at 900°C shows several distinctive features. The sharp and intense band with maxima at 3640 cm^{-1} appears in the spectrum and is assigned to the structural O–H anion (Garskaite et al., 2014), this indicates rearrangements in crystal structure of calcium phosphate upon annealing (Uskoković et al., 2018). Observed broadening and slight shifts of bands in the 1190-900 cm^{-1} region further confirms transformations between material phases (Querido et al., 2020). One can also observe that the intensity of overlapped bands assigned for the carbonate group decreases. This agrees with TG-FTIR gas analysis when the evolution of CO_2 and CO molecular species was observed upon calcining as-received powders at higher temperatures (Fig. 2). IR spectra indicate that the composition of fish-farming waste can be altered significantly by heat treatment leading to products that inhibit ignition of the main combustible components of wood, i.e. hemicellulose, lignin and cellulose.

XRD patterns of solid waste powders calcined at 550 °C and 900 °C are presented in Fig. 4. Evidently, the calcined material contains a mixture of crystalline compounds and the annealing at higher temperatures increase crystallinity and induce phase transformation. The main Bragg reflections in XRD patterns at 2θ = 32.53°, 35.5°, 38.7°, 39.2°, 36.3°, 48.7°, 53.5°, 58.3°, 61.6°, 61.8°, 66.3° and 68.1° were assigned to the (110), (002, $11\bar{1}$), (111), (200), ($\bar{1}12$), ($20\bar{2}$), (020), (202), ($\bar{1}13$), (022), ($31\bar{1}$) and (113) diffraction peaks of the CuO (ICDD card # 96-101-1195, monoclinic crystal system, space group of *C*2/c) phase (Palussière et al., 2019; Bulavchenko et al., 2019), confirming the presence of the Cu in the discharged waste material. Annealing at higher temperatures increased crystallinity, as evident by diffractograms showing small narrowing of the peaks assigned to the CuO phase. Other phases were also observed. From the patterns a series of small reflections at 2θ = 24.1°, 33.1°, 39.2°, 40.9°, 49.5°, 54.0°, 57.5°, 57.6°, 62.4° and 64.0° were assigned to the (110), (211), (222), (210), (202), (312), ($21\bar{1}$), (332), (310) and ($2\bar{1}\bar{1}$) diffraction peaks of the Fe_2O_3 (hematite, ICDD card # 96-101-1268, trigonal crystal system, space group of R-3c) (Raudoniene et al. 2018; Cheng et al. 2008). The signals at 2θ = 30.1°, 35.5°, 43.1°, 47.2°, 53.4°, 57.1° and 62.8° could be assigned to the diffraction peaks of the Fe_3O_4 (magnetite, ICDD card # 96-151-3302, space group Fd-3m, cubic crystal system) phase (Cheng et al., 2008; Liu et al., 2003). In the XRD pattern of waste material annealed at 550°C strong reflection at 2θ = 29.3° is present and it was assigned to the characteristic (104) diffraction peak of the $CaCO_3$ (calcite, ICDD card # 96-154-7349, trigonal crystal system, space group of R-3c) phase. Other small peaks corresponding to the calcite were also identified, i.e., reflections at 2θ = 36.0°, 39.4°, 43.2°, 47.0°, 47.5°, 48.5°, 57.4° and 60.7° were assigned to the (110), (113), (202), (204), (108), (116), (212) and (214) peaks. In the XRD pattern of the material annealed at 900°C the main reflection of the calcite at 2θ = 29.3° was absent and this can be attributed to its thermal decomposition and formation of the CaO (Rodriguez-Navarro et al., 2009). In this pattern, the small signal at 2θ = 37.4° was detected and assigned to the characteristic (200) peak of the CaO (ICDD card # 96-900-6695, cubic crystal system, space group of Fm-3m). Other small signals at 2θ = 32.2°, 53.8°, 64.1° and 67.4° of the CaO phase is also detected. The thermally induced structural phase transformation via a solid-state mechanism and thermal decomposition of the $CaCO_3$ has previously been reported (Koga et al., 2013; Yoshioka and Kitano, 1985). Furthermore, XRD patterns suggest annealed waste material contains small fraction of carbonated calcium phosphate mixture showing the main reflections in the region of 2θ = 31-34°. The signals of phases of different carbonated-hydroxyapatite (cHAP) (ICDD card no. 96-900-3552,

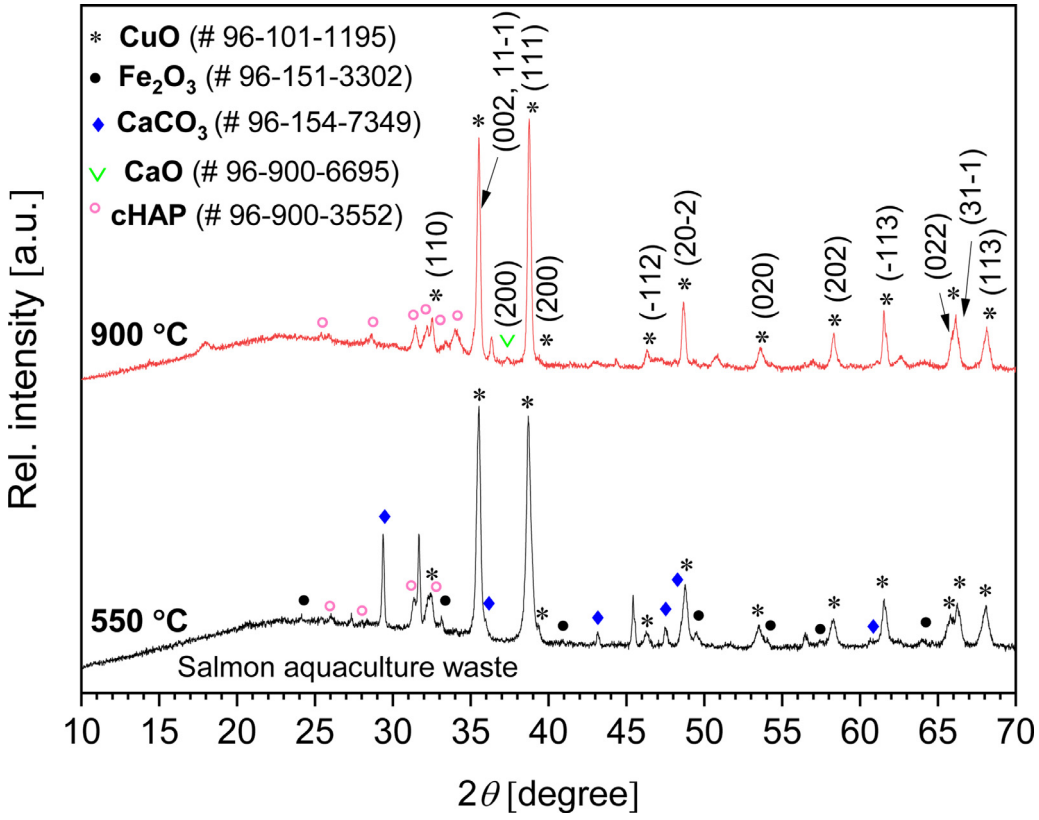

Fig. 4. XRD patterns of solid aquaculture as-received waste calcined at 550°C and 900°C. (Elevation of the background at $2\theta \approx 17\text{-}25^{\circ}$ is due to the glass sample holder).

ICDD card # 96-900-6695) may also be distinguished. Small changes in the intensities of the peaks in the XRD pattern of material annealed at 900°C can be attributed to the increase in crystallinity and material phase transformation (Garskaite et al., 2014; Garskaite et al., 2016). This also agrees with TG-FTIR absorption spectra when above 700°C the evolution of CO_2 gasses was observed. One shall also note that some reflections of the CuO, Fe_2O_3, $CaCO_3$, CaO and calcium phosphate different phases are overlapped, and further analyses are needed to estimate precise amount and ratios of constituents. Small elevation of the background ($2\theta \approx 17\text{-}25^{\circ}$) in the diffractograms was due to amorphous nature of the glass sample holder.

Camera photo and FE-SEM images showing surface morphological features of as-received waste powder and that of calcined at 550 ºC and 900 ºC are presented in Fig. 5. It can be observed that unprocessed material (Fig 5a,b) consist of agglomerated irregular particles of various dimeter and length with sizes in the range of about 100-300 μm. The higher magnification FE-SEM images of calcined powder material showed inhomogeneous morphology of agglomerates consisting of smaller primary particles with sizes in the range of several hundred nanometers (Fig. 5c). Further annealing at 900 ºC resulted in particle growth and formation of distinguishable crystals having sizes of ~10-20 μm (Fig. 5d). The morphology varied across the sample and this indicate that different constituents most likely form differently shaped particles and crystals, and this could hinder their diffusion into the wood matrix via pressure impregnation (Garskaite et al., 2019).

Elemental composition of waste material was studied by EDS, and analysis showed multielement content of aquaculture waste. The main elements detected were C, O, Cu and Ca. Other elements such as Na, Mg, Al, Si, P, S, Cl and Fe were also observed. The Cu concentration was high, i.e. ~ 18, 23 and 27 wt.% for the as-received and calcined at 550°C and 900°C material, respectively (data not presented). One shall also note that the distribution and content of elements varied notably within the different regions examined, indicating the presence of different phases formed. The EDS spectrum of the representative powder sample calcined at 550°C showing full composition of studied material as well as SEM image of place examined are presented in Fig. 6. Analysis showed that the relative wt% of Cu, Fe, Ca increased upon annealing while wt% of C decreased. This can be attributed to the thermal degradation of organic matter present within waste biomass, which decomposes into CO_2 and H_2O upon heating. SEM/EDS results agree with XRD data when the main phase of CuO, Ca containing compounds and Fe_2O_3 were identified. Results also indicate that other detected elements might be incorporated within crystal lattice of different phases and so forming solid solutions upon annealing (Sunde et al., 2012; Kizalaite et al., 2021). Furthermore, literature reports showed that elements detected within aquaculture waste material comprise the inorganic chemical substances that delay the ignition and the reduction of heat and combustion rate (Liodakis et al., 2006). Metals, such as Cu and Fe, are expected to absorb heat and so preventing the ignition of wood constituents. To an even greater extend, the incorporation of copper into formulations would be beneficial for wood preservation against biological degradation, which is an important factor defining life expectancy of wood products. The Nordic wood preserving industry produces around 2.1 million m^3 of preservative-treated wood per year, which is about one third of the total supply of preservative-treated wood in Europe (Salminen et al., 2014). This further indicates a pressing need for innovative solutions on how the active components against biodegradation can be transformed into a valuable product throughout the demand for circularity and sustainable industry.

TEM analysis was further performed to evaluate the sizes of primary particles within the agglomerates of fish-farming waste material calcined at 550°C, and the TEM images are presented in Fig. 7. The particles appear to be clustered and consisting of individual smaller particles of 50-100 nm sizes (Figs. 7a and b). Material composition, structure,

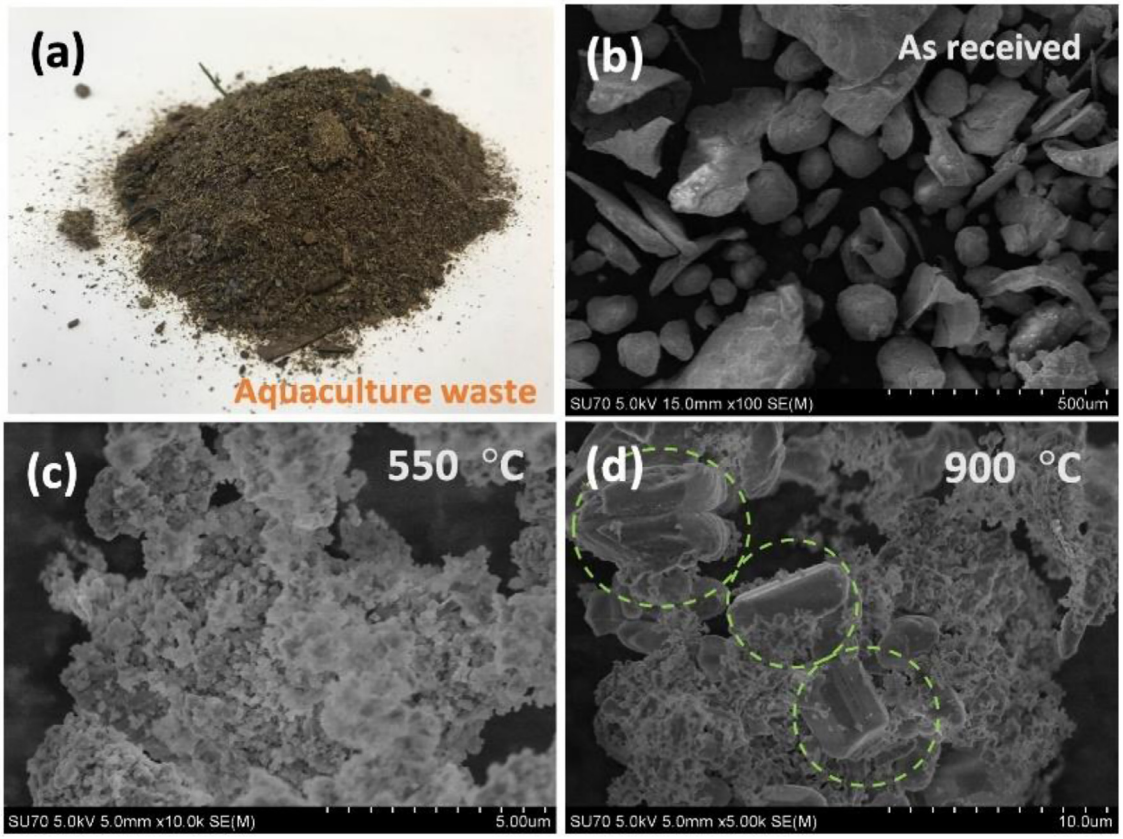

Fig. 5. Camera image (a) of as-received aquaculture waste powders, and FE-SEM images of (b) as-received waste powders and calcined at (c) 500 °C and (d) 900 °C (formed different size crystals are marked in green circles).

as well as processing parameters influence morphology of the resultant material. During the calcination, the reduction in particle boundaries and porosity occurs at higher temperatures, which leads to the particle and grain growth. Furthermore, the distinguished primary particles of the calcined waste material were measured to be as small as ~5 nm in sizes (Fig. 7c). This indicates that such nanoscale particles shall be able to diffuse into wood cell lumina (Garskaite et al., 2019), if accurate wood impregnation procedures were developed.

3.2. Cone-calorimeter studies

The fire behaviour of untreated wood and that of treated with aquaculture waste (as-received and calcined at 550°C) was evaluated by performing cone calorimeter testing, and the heat release rate (HRR) curves are displayed in Fig. 8. Aquaculture waste calcined at 900°C possess larger particles/crystals, as confirmed by XRD (Fig. 4) and SEM (Fig 5), that leads to their different movement, i.e. faster sedimentation, in the solution and associated flow into the wood matrix during the impregnation process. Whereas the diffusion of small particles into wood matrix and cell wall accessibility under specific condition is known (Garskaite et al., 2021; Guo et al., 2020). Based on this concept, we used as-received and calcined at 550°C aquaculture waste to study behaviour of wood fire-retardancy. The HRR of the untreated Scots pine wood (Fig 8) is typical of that reported in the literature (Lin et al., 2021). The treated wood behaves similar to the untreated wood, and only small changes in combustion behaviour was observed. The addition of as-received waste showed a small increase in the first peak HRR, while addition of calcined material resulted in a marginal reduction in the first peak HRR, and this could be attributed to the constituents of aquaculture waste material. The small decrease in the first peak HRR of the samples treated with the calcined waste could indicate fire-retardant

Table 1
Cone calorimeter data of untreated and treated samples[a].

sample	Density [kg/m^3]	TTI [s]	pHRR [kW m^{-2}]	THR [MJ m^{-2}]
Untreated Scots pine sapwood				
sample (1)	530.2	54	255	75
sample (2)	536.9	57	231	80
Wood treated with aquaculture waste				
as-received (1)	533.4	57	263	79
as-received (2)	535.3	60	281	79
as-received (3)	539.2	59	270	76
Wood treated with calcined waste				
550°C (1)	489.5	35	241	71
550°C (2)	449.4	47	222	67
550°C (3)	525.4	44	241	71

[a] TTI, time to ignition; pHRR, peak heat release rate; THR, total heat release.

effect of oxide-based materials present in the processed waste. One can also observe that two wood samples treated with the calcined material exhibited HRR curves with second peak HRR shifted to shorter exposure time, i.e. the maxima of a second peak was observed at a time of 440 s after the ignition of the specimens, that is 80 s earlier compared to the other tested samples. This can be attributed to the intrinsic properties of wood material; the density of these wood samples was significantly lower compared to those calculated for the other specimens (density values are presented in Table 1). The heterogeneity of wood material and high variability of properties within a single tree are well reported in the literature (Wasik et al., 2020; Schonfelder et al., 2019; Schonfelder et al., 2017; Tomczak et al., 2007). The time from the start of irradiation to ignition (TTI) for the different specimens show a very small delay for wood specimens treated with as-received waste compared to the untreated ones. However, the TTI for the wood treated with waste cal-

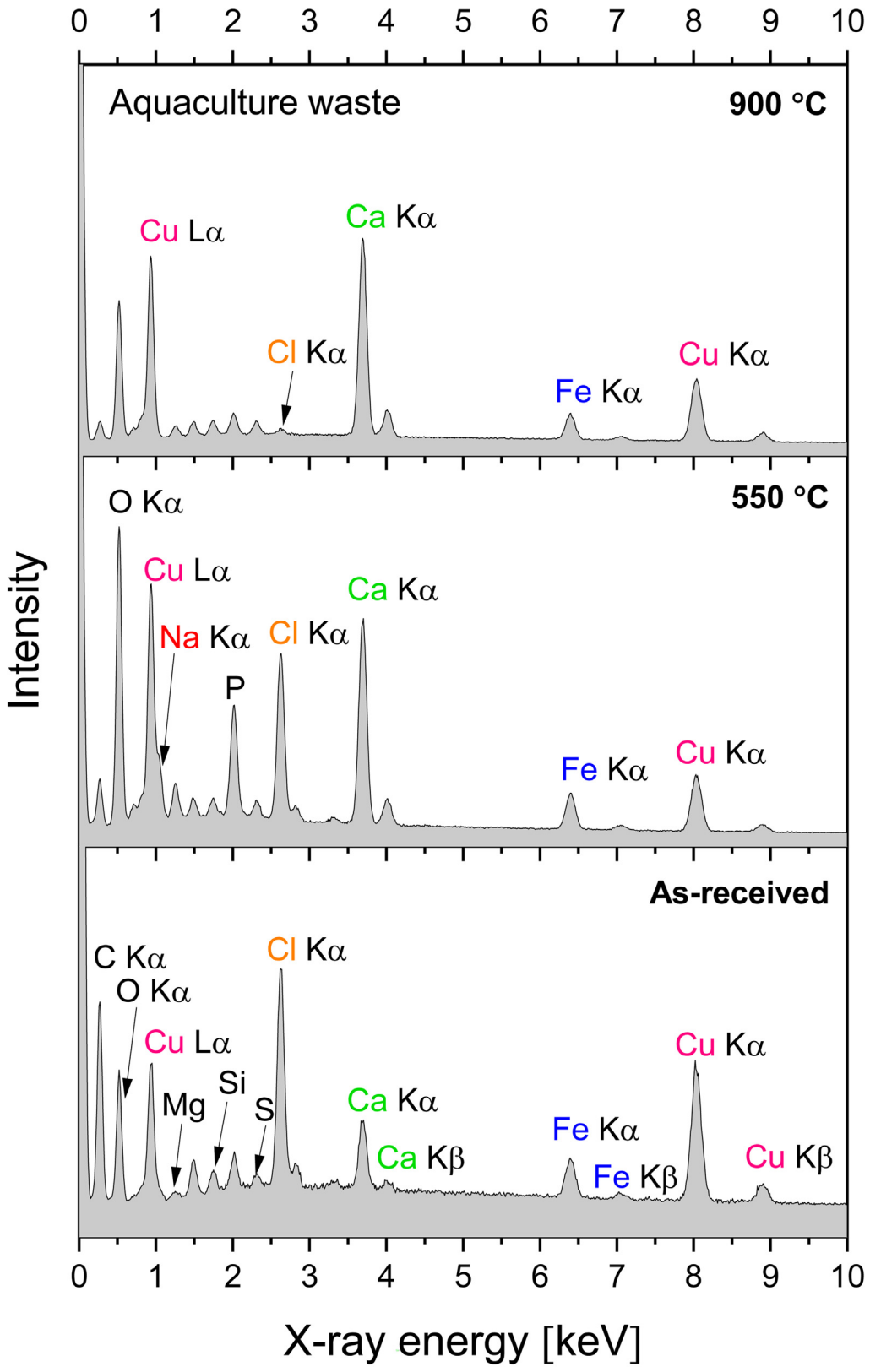

Fig. 6. EDS spectra of the aquaculture waste material (as-received, and annealed at 550°C and 900°C) showing multielement composition.

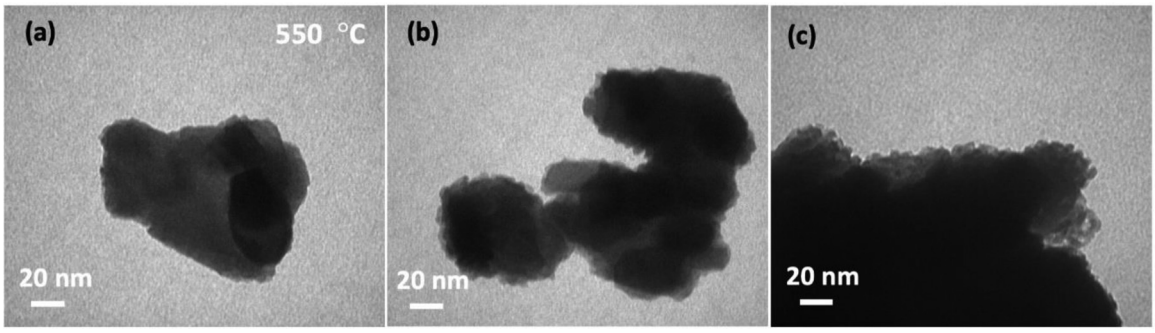

Fig. 7. TEM images of the aquaculture waste material annealed at 550°C showing agglomerated primary particles.

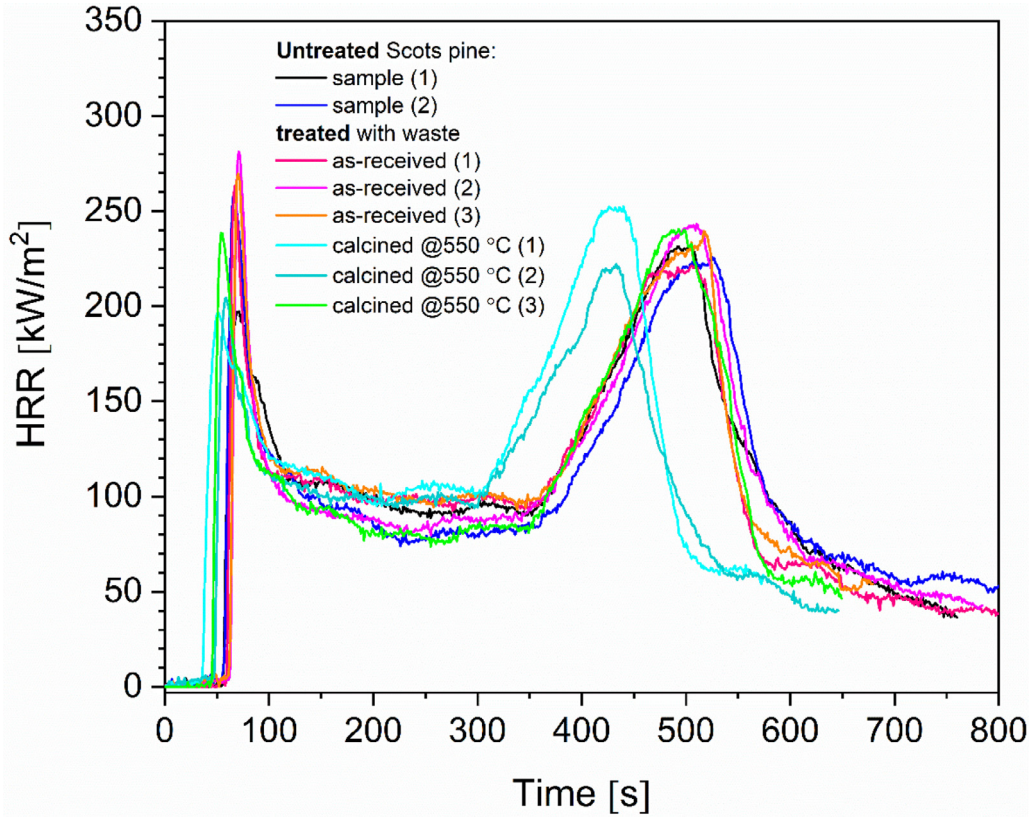

Fig. 8. Cone calorimeter results of the heat release rate (HRR) of untreated Scots pine and wood treated with as-received aquaculture waste and treated with waste annealed at 550°C.

cined at 550°C was slightly reduced, and this could be attributed to the different surface properties due to the treatment and constituents of the waste material. Overall, time to ignition depends on material properties, such as density, thermal conductivity, specific heat capacity, moisture content, surface properties and grains orientation (Babrauskas, 2002) as well as emissivity (Wickström, 2016) and ignition temperature of the material. Kirchhoff's law states that the emissivity of a body (or surface) equals its absorptivity on spectral level. Treated samples exhibited darker colour (Fig. 9) due to the presence of Cu and Fe oxides. These materials possess different heat absorption properties compared to the pure wood, and, therefore, more heat will be absorbed by the surface which subsequently could lead to an increased surface emissivity of the sample. Furthermore, adding the inorganic material might resulted in the different moisture/water presence on the wood surface which alters dehydration of the sample and flammability properties (Lowden and Hull, 2013). The THR curves shown in Fig. 10 are consistent with the HRR data. Inset in Fig. 10 shows representative sample of the Scots pine wood treated with the calcined waste at 550°C before and after the cone calorimeter test. The main parameters, including time to ignition (TTI), peak heat release rate (pHRR), and total heat release (THR), evaluated during the cone calorimetry tests are summarised in Table 1. The samples exhibited similar curves of the mass loss and the mass loss rate (data not shown), and the average residue mass after the combustion (about 650 s from the beginning of the experiment) resulted in residue mass between 15.42 % to 20.47 %.

Overall results indicate that further studies such as exploring the infiltration of oxide-based material into the deeper wood matrix layers are needed (Garskaite et al., 2021). The development of colloidal formulations that could diffuse into the wood matrix using industrial pressure techniques might be an alternative route to achieve desired properties of synergistic effects of inorganic-based compounds and wood material.

Fig. 9. Camera photos of untreated Scots pine and that of the treated with as-received and annealed at 550°C aquaculture waste material showing different colour of the wood surface due to the deposited material.

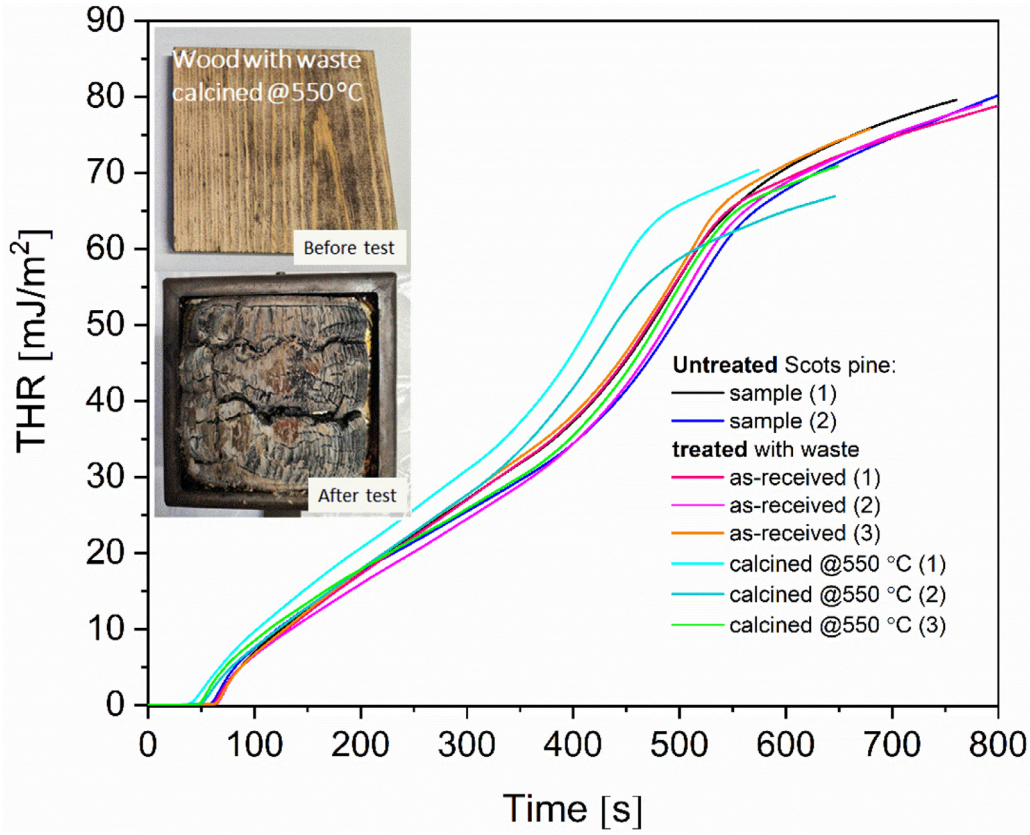

Fig. 10. Cone calorimeter results of the total heat release rate (THR) curves of untreated Scots pine and wood treated with as-received and annealed at 550°C aquaculture waste material (Inset: Representative sample of the Scots pine wood showing radial section (RL-plane) treated with the calcined waste at 550°C before and after the cone calorimeter test).

4. Conclusions

In this work, dried-solid waste material from the fish-farms net-cleaning process was evaluated as a fire-retardancy promoter for Scots pine sapwood. TG-FTIR gas analysis of as-received waste material indicated that the process progressed via the three main steps attributed to removal of adsorbed water, decomposition of organic matter subjected to pyrolysis, and decomposition of inorganics upon annealing material at higher temperatures. Morphology studies revealed calcined material consisting of agglomerated particles and crystals of various sizes. SEM/EDX analysis further revealed multi-elemental composition, and average copper contents of 14, 19 and 18 wt.% were calculated for the as-received material and the material calcined at 550°C and 900°C, respectively. XRD analysis revealed multiphase composition and the main crystalline phases of CuO, Fe_2O_3, $CaCO_3$ and carbonated-hydroxyapatite were detected of the calcined waste material. IR spectra revealed that as-received waste consisted of organic and inorganic substances and that the high-temperature annealing treatment induced the formation of low crystallinity cHAP phase. Cone-calorimeter tests showed very small decrease in the heat release rate for the Scots pine sapwood treated with waste material, indicating that an enhancement of the fire-retardancy properties occurred. Overall results showed that the generated waste discharge from net-cleaning facilities has potential to be used in the protection of wood against fire, and thus, via value-creation, to promote the pathway towards the responsible use of materials, cost-effective and environmentally sustainable solutions.

Declaration of Competing Interest

The authors declare that they have no known competing financial interests or personal relationships that could have appeared to influence the work reported in this paper.

Acknowledgement

The study was funded by the Swedish Research Council FORMAS project “Utilization of solid inorganic waste from the aquaculture industry as wood reinforcement material for flame retardancy” (grant no. 2018-01198). Glenn Mo (Egersund Net, AKVA group, Norway) and team of Global Enviro AS, Norway, are greatly acknowledged for valuable discussions and providing the fish-farming waste from washing stations. Maria M. Estevez acknowledges support from COWIfonden for the writing and editing of the manuscript. Mr. Chia-feng Lin (LTU) is acknowledged for processing raw sapwood blocks ($10 \times 10 \times 1$ cm^3) used for cone-calorimeter measurements.

References

Babrauskas, V., 2002. Ignition of wood: A review of the state of the art. J. Fire Prot. Eng. 12, 163–189.
Bailey, J.L., Eggereide, S.S., 2020. Mapping actors and arguments in the Norwegian aquaculture debate. Mar. Policy 115, 103898.
Bannister, J., Sievers, M., Bush, F., Bloecher, N., 2019. Biofouling in marine aquaculture: a review of recent research and developments. Biofouling 35, 631–648.
Bloecher, N., Floerl, O., 2020. Efficacy testing of novel antifouling coatings for pen nets in aquaculture: How good are alternatives to traditional copper coatings? Aquaculture 519, 734936.
Bloecher, N., Floerl, O., 2021. Towards cost-effective biofouling management in salmon aquaculture: a strategic outlook. Reviews in Aquaculture 13, 783–795.
Bosch Reig, F., Gimeno Adelantado, J.V., Moya Moreno, M.C.M., 2002. FTIR quantitative analysis of calcium carbonate (calcite) and silica (quartz) mixtures using the constant ratio method. Application to geological samples. Talanta 58, 811–821.
Braithwaite, R.A., Cadavid Carrascosa, M.C., McEvoy, L.A., 2007. Biofouling of salmon cage netting and the efficacy of a typical copper-based antifoulant. Aquaculture 262, 219–226.
Bulavchenko, O.A., Vinokurov, Z.S., Saraev, A.A., Tsapina, A.M., Trigub, A.L., Evgeny Yu Gerasimov, E.Y., Gladky, A.Y, Fedorov, A.V., Yakovlev, V.A., Kaichev, V.V., 2019. The influence of Cu and Al additives on reduction of iron(III) oxide: in situ XRD and XANES study. Inorg. Chem. 58, 4842–4850.
Carballeira Braña, C.B., Cerbule, K., Senff, P., Stolz, I.K., 2021. Towards environmental sustainability in marine finfish aquaculture. Frontiers in Marine Science 8, 666662.
Cebi, N., Durak, M.Z., Toker, O.S., Sagdic, O., Arici, M., 2016. An evaluation of Fourier transforms infrared spectroscopy method for the classification and discrimination of bovine, porcine and fish gelatins. Food Chem. 190, 1109–1115.
Chen, L., Wang, Y.Z., 2010. A review on flame retardant technology in China. Part 1: development of flame retardants. Polym. Adv. Technol. 21, 1–26.
Chen, M.-J., Lin, Y.-C., Wang, X.-N., Zhong, L., Li, Q.-L., Liu, Z.-G., 2015. Influence of cuprous oxide on enhancing the flame retardancy and smoke suppression of epoxy resins containing microencapsulated ammonium polyphosphate. Ind. Eng. Chem. Res. 54, 12705–12713.
Cheng, C.-J., Lin, C.-C., Chiang, R.-C., Lin, C.-R., Lyubutin, I.-S., Alkaev, E.-A., Lai, H.-Y., 2008. Synthesis of monodisperse magnetic iron oxide nanoparticles from submicrometer hematite powders. Cryst. Growth Des. 8, 877–883.
Comas, J., Parra, D., Balasch, J.C., Tort, L., 2021. Effects of fouling management and net coating strategies on reared gilthead sea bream juveniles. Animals 11 (3), 734.
Eimontas, J., Yousef, S., Striūgas, N., Abdelnaby, M.-A., 2021. Catalytic pyrolysis kinetic behaviour and TG-FTIR-GC–MS analysis of waste fishing nets over ZSM-5 zeolite catalyst for caprolactam recovery. Renewable Energy 179, 1385–1403.
Estevez, M.M., Sapci, Z., Linjordet, R., Morken, J., 2014. Incorporation of fish by-product into the semi-continuous anaerobic co-digestion of pre-treated lignocellulose and cow manure, with recovery of digestate’s nutrients. Renewable Energy 66, 550–558.
Gallo, E., Schartel, B., Braun, U., Russo, P., Acierno, D., 2011. Fire retardant synergisms between nanometric Fe_2O_3 and aluminum phosphinate in poly(butylene terephthalate). Polym. Adv. Technol. 22, 2382–2391.
Garskaite, E., Alinauskas, L., Drienovsky, M., Krajcovic, J., Cicka, R., Palcut, M., Jonusauskas, L., Malinauskas, M., Stankeviciute, Z., Kareiva, A., 2016. Fabrication of a composite of nanocrystalline carbonated hydroxyapatite (cHAP) with polylactic acid (PLA) and its surface topographical structuring with direct laser writing (DLW). RSC Adv. 6, 72733–72743.
Garskaite, E., Karlsson, O., Stankeviciute, Z., Kareiva, A., Jones, D., Sandberg, D., 2019. Surface hardness and flammability of Na_2SiO_3 and nano-TiO_2 reinforced wood composites. RSC Adv. 9, 27973–27986.
Garskaite, E., Gross, K.-A., Yang, S.-W., Yang, T.C.-K., Yang, J.-C., Kareiva, A., 2014. Effect of processing conditions on the crystallinity and structure of carbonated calcium hydroxyapatite (CHAp). CrystEngComm 16, 3950–3959.
Garskaite, E., Stoll, S.L., Forsberg, F., Lycksam, H., Stankeviciute, Z., Kareiva, A., Alberto Quintana, A., Jensen, C.J., Liu, K., Sandberg, D., 2021. The accessibility of the cell wall in Scots pine (*Pinus sylvestris* L.) sapwood to colloidal Fe_3O_4 Nanoparticles. ACS Omega 6, 21719–21729.
Guo, H.Z., Ozparpucu, M., Windeisen-Holzhauser, E., Schleputz, C.M., Quadranti, E., Gaan, S., Dreimol, C., Burgert, I., 2020. Struvite mineralized wood as sustainable building material: mechanical and combustion behavior. ACS Sustain. Chem. Eng. 8, 10402–10412.
Hamdani, S., Longuet, C., Perrin, D., Lopez-cuesta, J.-M., Ganachaud, F., 2009. Flame retardancy of silicone-based materials. Polym. Degrad. Stab. 94, 465–495.
Hanserud, O.S., Lyng, K.-A., De Vries, J.W., Øgaard, A.F., Brattebø, H., 2017. Redistributing phosphorus in animal manure from a livestock-intensive region to an arable region: exploration of environmental consequences. Sustainability 9 (4), 595.
Huggett, C., 1980. Estimation of rate of heat release by means of oxygen consumption measurements. Fire Mater. 4, 61–65.
Ihli, J., Wong, W.C., Noel, E.H., Kim, Y.-Y., Kulak, A.N., Christenson, H.K., Duer, M.J., Meldrum, F.C., 2014. Dehydration and crystallization of amorphous calcium carbonate in solution and in air. Nat. Commun. 5, 3169.
Ishita, A., Dauksas, E., Remme, J.F., Richardsen, R., Anne-Kristin Løes, A.-K., 2020. Fish and fish waste-based fertilizers in organic farming – With status in Norway: A review. Waste Manage. (Oxford) 115, 95–112.
Kannan, S., Gariepy, Y., Raghavan, V., 2015. Optimization of enzyme hydrolysis of seafood waste for microwave hydrothermal carbonization. Energy Fuels 29, 8006–8016.
Khiari, Z., Kaluthota, S., Savidov, N., 2019. Aerobic bioconversion of aquaculture solid waste into liquid fertilizer: effects of bioprocess parameters on kinetics of nitrogen mineralization. Aquaculture 500, 492–499.
Kim, S.-S., Jeon, J.-K., Park, Y.-K., Kim, S., 2005. Thermal pyrolysis of fresh and waste fishing nets. Waste Manage. (Oxford) 25, 811–817.
Kizalaite, A., Grigoraviciute-Puroniene, I., Asuigui, D.R.C., Stoll, S.L., Cho, S.H., Sekino, T., Kareiva, A., Zarkov, A., 2021. Dissolution–precipitation synthesis and characterization of zinc whitlockite with variable metal content. ACS Biomaterials Science & Engineering 7, 3586–3593.
Koga, N., Kasahara, D., Kimura, T., 2013. Aragonite crystal growth and solid-state aragonite–calcite transformation: a physico–geometrical relationship via thermal dehydration of included water. Cryst. Growth Des. 13, 2238–2246.
Laoutid, F., Vahabi, H., Movahedifar, E., Laheurte, P., Vagner, C., Cochez, M., Brison, L., Reza Saeb, M., 2021. Calcium carbonate and ammonium polyphosphate flame retardant additives formulated to protect ethylene vinyl acetate copolymer against fire: hydrated or carbonated calcium? J. Vinyl Add. Tech. 27, 264–274.
Lazar, S.T., Kolibaba, T.J., Grunlan, J.C., 2020. Flame-retardant surface treatments. Nat. Rev. Mater. 5, 259–275.
Lin, C.-f., Karlsson, O., Martinka, J., Rantuch, P., Garskaite, E., Mantanis, G.I., Jones, D., Sandberg, D., 2021. Approaching highly leaching-resistant fire-retardant wood by in situ polymerization with melamine formaldehyde resin. ACS Omega 6, 12733–12745.
Liodakis, S., Vorisis, D., Agiovlasitis, I.P., 2006. Testing the retardancy effect of various inorganic chemicals on smoldering combustion of Pinus halepensis needles. Thermochim. Acta 444, 157–165.
Lippke, B., Wilson, J., Meil, J., Taylor, A., 2010. Characterizing the importance of carbon stored in wood products. Wood Fiber Sci. 42, 5–14.
Liu, K., Zhao, L., Klavins, P., Osterloh, F.E., Hiramatsu, H., 2003. Extrinsic magnetoresistance in magnetite nanoparticles. J. Appl. Phys. 93, 7951–7953.
Lowden, L.A., Hull, T.R., 2013. Flammability behaviour of wood and a review of the methods for its reduction. Fire Science Reviews 2 (1), 4.
Merk, V., Chanana, M., Keplinger, T., Gaan, S., Burgert, I., 2015. Hybrid wood materials with improved fire retardance by bio-inspired mineralisation on the nano- and submicron level. Green Chem. 17, 1423–1428.
Norwegian Agriculture Agency (Landbruksdirektoratet), 2018. https://www.landbruksdirektoratet.no/nb/jordbruk/miljo-og-klima.
Norwegian Food Safety Authority (Mattilsynet). 2019. Veiledning til forskrift 4. juli 2003 nr. 951 om gjødselvarer mv. av organisk opphav.
Norwegian Scientific Committee for Food Safety (VKM) 2010. Assessment of the Fish Silage Processing Method (FSPM) for treatment of category 2 and 3 material of fish origin.
Östman, B.A.L., Tsantaridis, L.D., 2017. Durability of the reaction to fire performance of fire-retardant-treated wood products in exterior applications – a 10-year report. International Wood Products Journal 8, 94–100.
Östman, B., 2021. National fire regulations for the use of wood in buildings – worldwide review 2020. Wood Mater. Sci. Eng. 1–4.
Palussière, S., Cure, J., Nicollet, A., Fau, P., Fajerwerg, K., Kahn, M.L., Estève, A., Rossi, C., 2019. The role of alkylamine in the stabilization of CuO nanoparticles as a determinant of the Al/CuO redox reaction. Phys. Chem. Chem. Phys. 21, 16180–16189.
Pondelak, A., Škapin, A.S., Knez, N., Knez, F., Pazlar, T., 2021. Improving the flame retardancy of wood using an eco-friendly mineralisation process. Green Chem. 23, 1130–1135.
Popescu, C.-M., Pfriem, A., 2019. Treatments and modification to improve the reaction to fire of wood and wood based products—An overview. Fire Mater. 44 (1), 100–111.
Querido, W., Shanas, N., Bookbinder, S., Oliveira-Nunes, M.C., Krynska, B., Pleshko, N., 2020. Fourier transform infrared spectroscopy of developing bone mineral: from amorphous precursor to mature crystal. Analyst 145, 764–776.
Raudoniene, J., Laurikenas, A., Kaba, M.M., Sahin, G., Morkan, A.U., Brazinskiene, D., Asadauskas, S., Seidu, R., Kareiva, A., Garskaite, E., 2018. Textured WO_3 and WO_3:Mo films deposited from chemical solution on stainless steel. Thin. Solid. Films 653, 179–187.
Rodriguez-Navarro, C., Ruiz-Agudo, E., Luque, A., Rodriguez-Navarro, A.B., Ortega-Huertas, M., 2009. Thermal decomposition of calcite: mechanisms of formation and textural evolution of CaO nanocrystals. Am. Mineral. 94, 578–593.

Salminen, E., Valo, R., Kohonen, M., Jernlås, R., 2014. Wood preservation with chemicals, Best Available Techniques (BAT). Nordic Coulcil of Ministers, Copenhagen, Denmark, TemaNord, p. 550 2014,ISBN 978-92-893-2828-9.
Schonfelder, O., Zeidler, A., Boruvka, V., Bilek, L., 2019. Impact of silvicultural measures on the quality of Scots pine wood part II. Effect of site. Wood Research 64, 789–798.
Schonfelder, O., Zeidler, A., Boruvka, V., Bilek, L., 2017. Influence of site conditions and silvicultural practice on the wood density of Scots pine (*Pinus sylvestris* L.) – a case study from the Doksy locality, Czech Republic. Journal of Forest Science 63, 457–462.
Skvorčinskienė, R., Striūgas, N., Navakas, R., Paulauskas, R., Zakarauskas, K., Vorotinskienė, L., 2019. Thermal analysis of waste fishing nets for polymer recovery. Waste Biomass Valorization 10, 3735–3744.
Sunde Løveng, T.O., Garskaite, E., Otter, B., Fossheim, H.E., Sæterli, R., Holmestad, R., Einarsrud, M.-A., Grande, T., 2012. Transparent and conducting ITO thin films by spin coating of an aqueous precursor solution. J. Mater. Chem. 22, 15740–15749.
Tomczak, A., Pazdrowski, W., Jelonek, T., Stypula, I., 2007. Vertical variability of selected macrostructural properties of juvenile wood organization in trunks of Scots pine (*Pinus Sylvestris* L.) trees. Acta Societatis Botanicorum Poloniae 76, 27–33.
Uskoković, V., Marković, S., Veselinović, L., Škapin, S., Ignjatović, N., Uskoković, D.P., 2018. Insights into the kinetics of thermally induced crystallization of amorphous calcium phosphate. Phys. Chem. Chem. Phys. 20, 29221–29235.
Vidal, L., Joussein, E., Colas, M., Cornette, J., Sanz, J., Sobrados, I., Gelet, J.L., Absi, J., Rossignol, S., 2016. Controlling the reactivity of silicate solutions: a FTIR, Raman and NMR study. Colloids Surf. A 503, 101–109.
Vongsvivut, J., Heraud, P., Zhang, W., Kralovec, J.A., McNaughton, D., Barrow, C.J., 2012. Quantitative determination of fatty acid compositions in micro-encapsulated fish-oil supplements using Fourier transform infrared (FTIR) spectroscopy. Food Chem. 135, 603–609.
Wasik, R., Michalec, K., Barszcz, A., Mudryk, K., 2020. Variability of selected macrostructure features, density and compression strength along the grain of the "Taborz" Scots pine wood (*Pinus Sylvestris* L.). Drewno 63 (205), 171–182.
Wickström, U., 2016. New formula for calculating time to ignition of semi-infinite solids. Fire Mater. 40, 464–471.
Xu, W., Zhang, B., Wang, X., Wang, G., Ding, D., 2018. The flame retardancy and smoke suppression effect of a hybrid containing $CuMoO_4$ modified reduced graphene oxide/layered double hydroxide on epoxy resin. J. Hazard. Mater. 343, 364–375.
Yoshioka, S., Kitano, Y., 1985. Transformation of aragonite to calcite through heating. Geochem. J. 19, 245–249.